COPS5 (Jab1) Protein Increases β Site Processing of Amyloid Precursor Protein and Amyloid β Peptide Generation by Stabilizing RanBP9 Protein Levels[*]

Hongjie Wang[‡], **Debleena Dey**[‡], **Ivan Carrera**[§], **Dmitriy Minond**[¶], **Elisabetta Bianchi**[∥], **Shaohua Xu**[**], **and Madepalli K. Lakshmana**[‡1]

From the [‡]*Section of Neurobiology and* [¶]*Peptide-based Therapeutics, Torrey Pines Institute for Molecular Studies, Port Saint Lucie, Florida 34987, the* [§]*Department of Neuroscience, Euroespes Biotechnology, Poligono de Bergondo, Nave F, 15165A, Coruna, Spain, the* [∥]*Immunoregulation Unit, Department of Immunology, Institut Pasteur, 25 rue du Dr. Roux, 75724 Paris, France, and the* [**]*Florida Institute of Technology, Melbourne, Florida 32901*

Background: Increased generation of toxic amyloid β peptide (Aβ) in the brain is central to the pathogenesis of Alzheimer's disease (AD).

Results: COPS5 (Jab1) is a novel RanBP9-interacting protein that robustly increases Aβ generation

Conclusion: COPS5 increases Aβ generation by stabilizing RanBP9 protein levels.

Significance: Lowering COPS5 levels may be an effective therapeutic approach for AD.

Increased processing of amyloid precursor protein (APP) and accumulation of neurotoxic amyloid β peptide (Aβ) in the brain is central to the pathogenesis of Alzheimer's disease (AD). Therefore, the identification of molecules that regulate Aβ generation is crucial for future therapeutic approaches for AD. We demonstrated previously that RanBP9 regulates Aβ generation in a number of cell lines and primary neuronal cultures by forming tripartite protein complexes with APP, low-density lipoprotein-related protein, and BACE1, consequently leading to increased amyloid plaque burden in the brain. RanBP9 is a scaffold protein that exists and functions in multiprotein complexes. To identify other proteins that may bind RanBP9 and regulate Aβ levels, we used a two-hybrid analysis against a human brain cDNA library and identified COPS5 as a novel RanBP9-interacting protein. This interaction was confirmed by coimmunoprecipitation experiments in both neuronal and non-neuronal cells and mouse brain. Colocalization of COPS5 and RanBP9 in the same subcellular compartments further supported the interaction of both proteins. Furthermore, like RanBP9, COPS5 robustly increased Aβ generation, followed by increased soluble APP-β (sAPP-β) and decreased soluble-APP-α (sAPP-α) levels. Most importantly, down-regulation of COPS5 by siRNAs reduced Aβ generation, implying that endogenous COPS5 regulates Aβ generation. Finally, COPS5 levels were increased significantly in AD brains and APΔE9 transgenic mice, and overexpression of COPS5 strongly increased RanBP9 protein levels by increasing its half-life. Taken together, these results suggest that COPS5 increases Aβ generation by increasing RanBP9 levels. Thus, COPS5 is a novel RanBP9-binding protein that increases APP processing and Aβ generation by stabilizing RanBP9 protein levels.

Alzheimer's disease (AD)[2] is an irreversible neurodegenerative disorder that presents with progressive intellectual deterioration involving memory, language, and judgment, ultimately leading to a total dependence on nursing care. It is now estimated that nearly 35.6 million patients are affected by AD worldwide and that about 4.6 million new cases are added each year, causing an enormous societal and economic burden (1). Accumulation of amyloid plaques made up of amyloid β peptide (Aβ), derived from amyloid precursor protein (APP) through the action of β and γ-secretases is a major hallmark of AD. Converging genetic, biochemical, and pathological evidence strongly indicates that Aβ plays an early and crucial role in AD pathogenesis (2). Additionally, it was discovered recently that the A673T coding mutation in APP protects significantly against memory decline in patients with AD as well as in the normally aging population by decreasing Aβ levels (3). These findings provided a significant boost to the role of APP metabolism as a cause of not only familial but also sporadic cases of AD.

AD is a multifactorial and heterogeneous disease that has been suggested to have a strong genetic basis with heritability estimates of up to 80% (4). Twin and family studies have confirmed that genetic factors are estimated to play a crucial role in at least 80% of AD cases (5). However, genetic variants in the four well established genes, namely APP, presenilin 1, presenilin 2, and ApoE, account for less than 1% of AD cases (6). If we combine these well established genes with the newly identified nine genetic risk factors from the genome-wide association studies for late-onset AD, they together account for only less than half of this heritability (7). Therefore, additional risk genes need to be identified. The recent failure of secretase inhibitors

[2] The abbreviations used are: AD, Alzheimer's disease; Aβ, amyloid β peptide; APP, amyloid precursor protein; SD, selective dropout; X-gal, 5-bromo-4-chloro-3-indolyl-β-D-galactopyranoside; CTF, C-terminal fragment; bis-tris, 2-[bis(2-hydroxyethyl)amino]-2-(hydroxymethyl)propane-1,3-diol; LRP, low-density lipoprotein receptor-related protein; NC, normal control; LFA, lymphocyte function-associated antigen 1; FL, full-length.

at the clinical trials because of unacceptable levels of toxicity also indicates the need for the identification of all proteins that regulate or modulate Aβ generation so that they may be targeted for novel designs in future therapeutic approaches.

RanBP9 is a scaffolding protein implicated in a variety of functions through integration of cell surface receptors with intracellular signaling targets (8). Recently, RanBP9 was found to be within the clusters of RNA transcript pairs associated with markers of AD progression, suggesting that RanBP9 might contribute to the pathogenesis of AD (9). In fact, even before this finding, we showed for the first time that RanBP9 protein levels are increased 6-fold in AD brains (10) and that RanBP9 overexpression increases Aβ generation 4-fold in cell cultures by increasing β-secretase-mediated processing of APP (11) and also increases amyloid plaques in mouse brains (12), which, in turn, leads to a significant loss of synaptic proteins (12). Because RanBP9 is known to exist in large multiprotein complexes of greater than 670 kDa (13, 14), we speculated that Aβ generation may be modulated by several other RanBP9-binding proteins. Therefore, we used RanBP9 as bait in a yeast two-hybrid screen and identified COP9 constitutive photomorphogenic homolog subunit 5 (COPS5) as a *bona fide* binding partner of RanBP9. We confirmed COPS5 binding to RanBP9 under overexpression conditions using tagged antibodies and also binding of endogenous proteins in HEK293 and NT2 cells as well as mouse brains. We also show here that COPS5 increases Aβ generation by stabilizing RanBP9 protein levels.

EXPERIMENTAL PROCEDURES

DNA Constructs—To subclone the bait constructs for the RanBP9-LisH and RanBP9-SPRY domains, PCR-amplified cDNA encoding the human RanBP9-LisH region (amino acids 365–397) and RanBP9-SPRY region (amino acids 213–365) were amplified using PcDNA3-FLAG-RanBP9 as a template. The amplified DNA was ligated into the NcoI-SalI restriction sites of the pGBKT7 vector (Clontech, Palo Alto, CA), resulting in the pGBKT7-LisH and pGBKT7-SPRY constructs. These bait cDNAs were cloned in-frame with the Gal4 DNA-binding domain. The CTLH domain of RanBP9 was also cloned into the pGBKT7 vector in the same NcoI-SalI restriction sites. FLAG-HA-COPS5 was a gift from Dr. Wade Harper (Addgene plasmid no. 22541). GFP-RanBP9-FL construct was received from Dr. Hideo Nishitani, Kyushu University, Japan. The Δ1, Δ2, and Δ3 GFP-RanBP9 deletion constructs were prepared by a combination of PCR amplification and restriction digestions. All of these cDNA constructs were sequence-verified, and protein expression was confirmed prior to use.

Chemicals and Antibodies—The minimal selective dropout (SD) base, minimal SD agar base, and dropout-Ade/-His/-Leu/-Trp supplement were all purchased from BD Biosciences. X-α-Gal (5-bromo-4-chloro-3-indolyl-a-D-galactopyranoside) was from Research Products International (Mt. Prospect, IL). Kanamycin solution was from Teknova (Hollister, CA). Ampicillin, adenine, leucine, tryptophan, histidine, salmon sperm double-stranded DNA (single-stranded DNA), and protease inhibitor mix for use in mammalian cells were from Sigma-Aldrich. The anti-mouse IgG-agarose beads and anti-rabbit IgG-agarose beads were from American Qualex International (San Clem-

ente, CA). The polyclonal antibodies CT15 (against the C-terminal 15 residues of APP) and 63d (against the APP ectodomain) have been described previously (11). The monoclonal antibody Ab9 used for immunoprecipitation of Aβ was purified from supernatants of the hybridoma generated in mice by Biomatik Corp. (Ontario, Canada). The monoclonal antibody 6E10 (catalog no. SIG-39300, recognizing 1–17 of the Aβ sequence) was obtained from Covance Research (Denver, CO). Polyclonal anti-sAPPβ-WT antibody (catalog no. 18957) was purchased from IBL Co. Ltd (Gunma, Japan). Monoclonal antibody against RanBP9 was produced by immunizing mice with a peptide corresponding to the 146–729 amino acids of RanBP9 as described previously (11). Anti-FLAG tag antibody (M2, catalog no. F3165) was purchased from Sigma. Anti-Jab1 rabbit monoclonal antibody (catalog no. 5156-1) was purchased from Abcam (Cambridge, MA). Mouse monoclonal anti-JAB1 antibody clone 2A10 (catalog no. NB120-495) was purchased from Novus Biologicals (Littleton, CO). Anti-BACE1 monoclonal antibody (catalog no. H00023621-Mo2) was obtained from Abnova (Taipei, Taiwan). The polyclonal antibody 1704 recognizing the cytoplasmic domain of human LRP has been described (11). Mouse monoclonal anti-gfp, clone N86/8, was obtained from Antibodies Inc. (University of California Davis, National Institutes of Health NeuroMab, Davis, CA). Mouse monoclonal antibody against β-actin (catalog no. A00702) was purchased from Genscript USA Inc. (Piscataway, NJ). All secondary antibodies were purchased from Jackson Immuno-Research Laboratories (West Grove, PA). All antibodies were diluted in 5% nonfat milk in Tris-buffered saline with 0.1% Tween 20 (TBS-T) buffer.

Yeast Two-hybrid Screen—The expression of the pGBKT7-LisH and pGBKT7-SPRY constructs was confirmed for protein expression by immunoblotting. Initially the constructs were tested for self-activation of the His3 reporter gene in the absence of the prey plasmid by plating transformed yeast on selective dropout plates lacking leucine and tryptophan. This was to rule out the possibility that the bait cDNA itself, in the absence of an interacting protein, might act as a transcriptional activator of the His gene. We used a high-stringency protocol to screen the library from human brain fused with the Gal4 trans-activation domain constructed in the PGADT7-T plasmid (Clontech). The yeast two-hybrid screening was performed in the AH109 yeast strain, which contains three reporters (ADE2, HIS2, and MEL1). The bait plasmid was initially transformed into AH109, and growth was selected in SD dropout plates lacking tryptophan as described previously (15). These yeast strains expressing the RanBP9-LisH or RanBP9-SPRY domains were then used individually for mating with the Tyr-187 mating strain transformed with a cDNA library made from human brain and plated them on SD dropout plates lacking adenine, histidine, leucine, and tryptophan. Yeast was allowed to grow for 72 h at 30 °C before His+ cells were scored and an X-gal (5-bromo-4-chloro-3-indolyl-β-D-galactopyranoside) overlay assay was performed. Colonies that grew under histidine (His+) were then tested for galactosidase expression. Colonies that were positive for both His+ and β-galactosidase (LacZ) were selected as first-round positives. The interactions were then verified by recovering prey plasmids from positive colo-

nies, transforming them into yeast strains expressing the RanBP9-LisH or RanBP9-SPRY domains as bait and reconfirming the HIS+ and LacZ+ phenotype. The plasmid DNAs from the yeast were shuttled to bacteria by standard methods and subjected to endonuclease restriction digest analysis to sort out both different and identical cDNA library plasmids. Different sizes of cDNA prey inserts from yeast that grew under selection were sequenced. The identities of the prey inserts were determined by Basic Local Alignment Search Tool comparison against the National Center for Biotechnology database.

Cell Cultures, Transient Transfections, and Immunoprecipitations—HEK293FT and human neuron-committed teratocarcinoma (NT2) cells were grown in Dulbecco's modified Eagle's medium containing 10% fetal bovine serum, 2 mM L-glutamine, 100 μg/ml penicillin, and 100 μg/ml streptomycin. For coimmunoprecipitations and APP metabolism studies, transient transfections were performed using Lipofectamine 2000 (Invitrogen) and Opti-MEM I (Invitrogen). Equal amounts of empty vectors were included to keep the overall DNA quantity constant for all experimental groups. Coimmunoprecipitations were carried out exactly as described previously (11). Forty-eight hours after the transfection, conditioned media were collected for the detection of Aβ and sAPPs, and the lysates were used for the detection of C-terminal fragments (CTFs) and APP holoprotein.

Quantitation of Aβ, CTFs, and sAPPs in NT2 Cells—After 48 h of transient transfections, the conditioned medium was collected, centrifuged to remove cell debris, and immunoprecipitated overnight using a monoclonal Ab9 antibody (recognizing the 1–16 amino acids of Aβ) to pull down total Aβ. After SDS-PAGE electrophoresis using NuPAGE 4–12% bis-tris gels, total Aβ was detected by immunoblotting using a mixture of 6E10/82E1 antibodies, which reliably detect total Aβ as described previously (10–12). The conditioned medium was also immunoblotted to detect sAPPα (6E10), sAPPβ (anti-sAPPβ-WT, and rabbit IgG; IBL America Ltd.) and sAPPtotal (63G) using the indicated antibodies. To detect APP holoprotein and CTFs, the cells were lysed using lysis buffer (1% Nonidet P-40) with complete protease inhibitor mix (Sigma), and equal amounts of proteins were loaded in to each well and subjected to SDS-PAGE electrophoresis. Following transfer onto PVDF membranes, they were blocked with 5% milk in TBS-T and incubated overnight with primary antibodies, followed by 1–4 h of incubation with HRP-conjugated secondary antibodies, such as monoclonal goat anti-mouse IgG light chain or polyclonal goat anti-rabbit IgG light chain. The protein signals were detected using Super Signal West Pico chemiluminescent substrate (Pierce). Quantitation of Western blot signals was done using Java-based ImageJ software available freely from the National Institutes of Health.

Aβ Detection by ELISA—We also used ELISA for detection of Aβ levels because of a significant reduction of COPS5 siRNAs that exceeded the detection limit of immunoblot analyses for Aβ. A 19-nucleotide siRNA duplex targeting COPS5 or RanBP9 and scrambled control siRNA were synthesized and supplied in a 2′-deprotected, annealed, and desalted format from Dharmacon (Lafayette, CO). The siRNAs were transiently transfected into neuro-2A (N2A) cells stably expressing the APP695swe

mutation at 50–100 nM final concentrations using Lipofectamine 2000 (Invitrogen), according to the instructions provided by the manufacturer. After 24 h of the first transfection, a second transfection was performed to enhance the knockdown effect of the siRNAs. Twenty-four hours after the second transfection, conditioned media were collected and centrifuged to remove the debris. Aβ was detected by sandwich ELISA exactly as described previously by our laboratory (11).

Immunocytochemistry—To localize endogenous proteins, anti-COPS5 or anti-RanBP9 antibodies were used either alone or together. The staining procedure was exactly as described previously (10) except that here we used a different type of cells.

Statistical Analysis—Immunoblot signals for Aβ, CTFs, sAPPs, APP holoprotein, COPS5, RanBP9, and actin were quantified using ImageJ software. Statistical significance was established by either Student's t test or analysis of variance followed by post hoc test using Instat3 software (GraphPad Software, San Diego, CA). We used a two-tailed p value, assuming that populations may have different standard errors. The data presented are mean ± S.E. The data were considered significant only if $p < 0.05$ (*, $p < 0.05$; **, $p < 0.01$; and ***, $p < 0.001$).

RESULTS

The RanBP9-LisH Domain Binds COPS5 in the Yeast Two-hybrid System—Recently, RanBP9 was found to be within the clusters of RNA transcript pairs associated with markers of AD progression, suggesting that RanBP9 might play a pathogenic role in AD (9). In fact, down-regulation of RanBP9 significantly reduced Aβ generation in primary neuronal cultures (11), implying that RanBP9 regulates Aβ generation. This novel finding led us to strongly believe that RanBP9 and RanBP9-binding proteins are excellent therapeutic targets for AD. Therefore, to identify novel RanBP9 functional modulators, we performed a yeast two-hybrid screening of a human brain cDNA library using the human RanBP9-LisH domain as well as the RanBP9-SPRY domain as bait. We used a stringent protocol (quadruple dropout plates) to reduce the number of false positives. Of more than 1 million clones screened, we identified several colonies that repeatedly tested positive by turning blue and growing on the quadruple dropout plates. Among them, we were particularly interested in a clone that turned out to contain the partial cDNA for the COP9 constitutive photomorphogenic homolog subunit 5 (COPS5, also called Jab1). Thus, yeast colonies that turned blue only when COPS5 was cotransformed with the RanBP9-LisH domain, but not when cotransformed with RanBP9-CTLH domain or when transformed with pGB-empty vector alone or with pGB-lamin used as a negative control, suggested a positive interaction between COPS5 and the RanBP9-LisH domain (Fig. 1A). The interaction between RanBP9-LisH and COPS5 was confirmed by quantitatively assaying for β-galactosidase activity using chlorophenol red-β-D-galactopyranoside as a substrate. Fig. 1B shows that the β-gal activity of RanBP9-LisH and COPS5 was 240 units ($p < 0.001$), almost comparable with the levels of 357 units ($p < 0.001$) for p53-T7, widely used as positive controls for Gal4-based yeast two-hybrid screens. The negative control, lamin, was only 37 units. Thus, RanBP9 binds COPS5 in the yeast two-hybrid system.
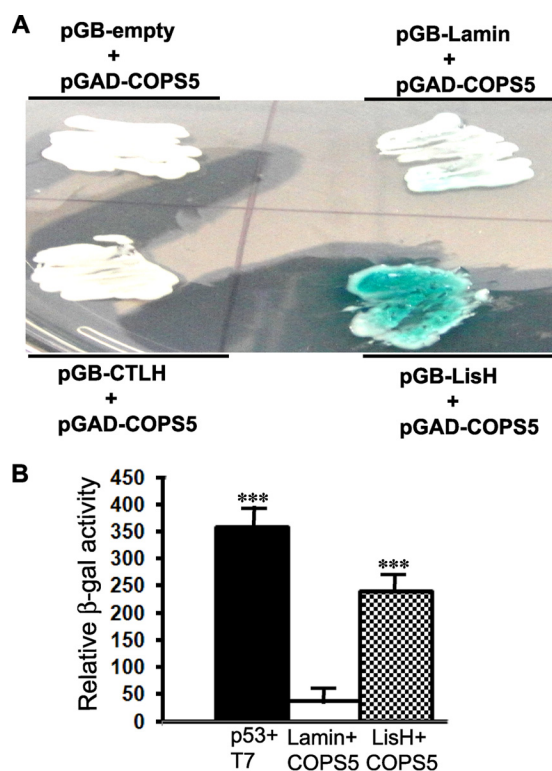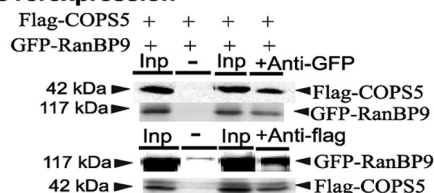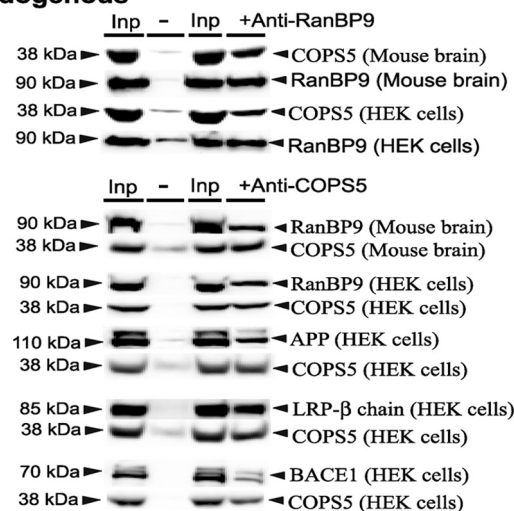
A

pGB-empty + pGAD-COPS5 | pGB-Lamin + pGAD-COPS5

pGB-CTLH + pGAD-COPS5 | pGB-LisH + pGAD-COPS5

B

FIGURE 1. **The RanBP9-LisH domain interacts with COPS5 (Jab1) in a yeast two-hybrid system.** *A*, after isolating COPS5 from the human brain cDNA library, pGB and pGAD vector combinations with or without COPS5, as mentioned in the figure, were cotransformed into the AH109 yeast strain, and resulting colonies were restreaked onto high-stringency plates containing kanamycin and X-gal. Robust growth and a change in color to blue indicated a physical interaction between the RanBP9-LisH domain and COPS5. *B*, quantitation of β-gal activity in liquid cultures of colonies transformed with pGB-RanBP9-LisH and pGAD-COPS5 demonstrated almost comparable levels to the widely used positive controls (p53 and T7), whereas the activity in the negative control (pGB-lamin) was negligible. One-way analysis of variance followed by post hoc Tukey-Kramer multiple comparisons test revealed significant differences. ***, $p < 0.001$. The data are mean ± S.E., and $n = 4$/group.

A. Overexpression

B. Endogenous

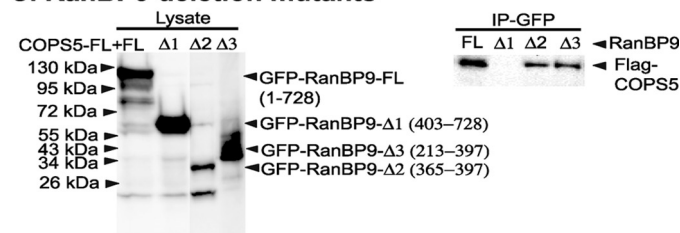### C. RanBP9 deletion mutants

FIGURE 2. **Overexpressed and endogenous COPS5 bind RanBP9 in HEK293FT cells and mouse brain by coimmunoprecipitations.** *A*, HEK293 cells were cotransfected with FLAG-COPS5 and GFP-RanBP9 vector combinations, as mentioned in the figure, and the lysates were subjected to immunoprecipitations with the indicated antibodies. FLAG-COPS5 was pulled down only when polyclonal antibody, anti-GFP, was included to precipitate GFP-RanBP9 (*upper panel*). Similarly, in the reciprocal immunoprecipitations, GFP-RanBP9 was pulled down only when the anti-FLAG antibody M2 was included (*lower panel*), confirming a physical interaction between RanBP9 and COPS5. The pulled-down proteins are compared with lysates used as inputs (*Inp*). The levels of GFP-RanBP9 and FLAG-COPS5 pulled down after immunoprecipitation with their respective antibodies are also shown. *B*, endogenous COPS5 was pulled down by monoclonal anti-RanBP9 antibody in both mouse brains (*upper panel*) and HEK293 cells (*lower panel*). Reciprocal immunoprecipitations also demonstrated a specific interaction between RanBP9 and COPS5 (*lower panel*). Anti-COPS5 antibody also pulled down APP (CT15), LRP-β chain (1704), and BACE1 (monoclonal anti-BACE1) in HEK cells. COPS5 protein pulled down with anti-COPS5 antibody is also shown for each immunoprecipitated protein. *C*, mapping of RanBP9 binding with COPS5 using RanBP9 deletion mutants. The *left panel* shows the protein expression of RanBP9-FL and deletion mutants at the bottom (the numbers in parenthesis indicate amino acid residues). The *right panel* shows that COPS5 was pulled down by RanBP9-FL, Δ2, and Δ3 mutants but not by Δ1. IP, immunoprecipitation.

RanBP9 Binds COPS5 in Cells and Mouse Brain—Next we used coimmunoprecipitation to confirm that the interaction occurs in a mammalian system. HEK293FT cells were cotransfected with cDNAs encoding FLAG- and HA-tagged COPS5 and GFP-tagged RanBP9. 150 μg of 1% Nonidet P-40 lysates were subjected to immunoprecipitation with anti-GFP antibodies. The immunoprecipitated complexes specifically contained FLAG-COPS5, which was detected by an anti-FLAG antibody (Fig. 2*A*). In the GFP-antibody minus controls, which contained only mouse IgG-agarose beads, FLAG-COPS5 was not detected. GFP-RanBP9 detected by GFP antibody is also shown. We further confirmed these interactions in the reciprocal coimmunoprecipitations, as shown in Fig. 2*A* (*lower panel*). Input (*Inp*) lysates corresponding to 150 μg of total proteins were loaded for comparison. Endogenous RanBP9 and COPS5 protein interactions were also confirmed in both HEK293 cells and mouse brain lysates. The 1% Nonidet P-40 lysates from HEK293 cells or mouse brains were ultracentrifuged, and the total proteins were quantified in the supernatants by the BCA method. Overnight incubation of equal amounts of protein lysates with polyclonal COPS5 antibody but not with control IgG beads specifically pulled down RanBP9 protein in HEK293 cells as well as mouse brains (Fig. 2*B*). These results confirmed

that not only the exogenous proteins but also endogenous RanBP9 and COPS5 interact with each other. Interestingly, immunoprecipitation with COPS5 antibody also pulled down APP (CT15), LRP-β chain (1704), and BACE1 (anti-BACE1) in HEK cells, suggesting that, like RanBP9, COPS5 also interacts directly with these proteins (Fig. 2*B*). COPS5 protein pulled
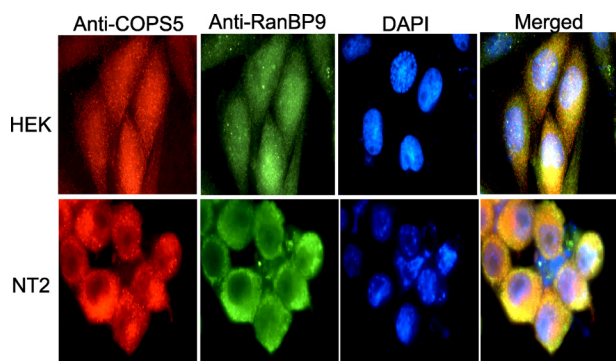
FIGURE 3. **Endogenous RanBP9 and COPS5 colocalize in HEK293 and NT2 cells.** HEK293 and NT2 cells were stained with monoclonal anti-RanBP9 and polyclonal COPS5 antibodies by immunocytochemistry. DAPI detected nuclei, and the merged images show a yellow color, demonstrating colocalization of endogenous RanBP9 and COPS5 in both HEK293 and NT2 cells.

down after immunoprecipitations with anti-COPS5 antibody is shown for both HEK cells and mouse brains (Fig. 2*B*).

The RanBP9-LIS1 Homology (LisH) Domain but Not the C-terminal to LisH (CTLH) and CT11-RanBP9 (CRA) Domains Bind COPS5—To map the domains within RanBP9 that bind to COPS5, we prepared different deletion mutants of RanBP9 as fusion proteins to GFP. These mutants were transiently cotransfected with FLAG-COPS5 in HEK293 cells and immunoprecipitated overnight with an anti-GFP antibody. The *left panel* of Fig. 2*C* shows the expression of proteins for the RanBP9-GFP deletion mutants. COPS5 was pulled down only when RanBP9 FL or the Δ2 or Δ3 mutants were cotransfected but not when Δ1 was cotransfected (Fig. 2*C*, *right panel*). This suggests that only the full-length or the LisH-SPRY domains of RanBP9, but not the CTLH and CRA domains, bind to COPS5.

RanBP9 and COPS5 Colocalize in the Same Subcellular Compartments—We demonstrated previously that the RanBP9 protein is present throughout the cytoplasm, including the complex neurite networks in the primary neuronal cultures and in the dendritic arbor in the adult mouse brain (12). Also, in our previous study, when COPS5 was transiently expressed in COS cells, COPS5 was found to be diffusely distributed throughout the cell (16). Although exogenous expression of proteins and staining for epitope-tagged proteins may provide some estimate for their localization, they do not reflect the absolute *in vivo* situation. Therefore, we next performed double immunostaining for the endogenous proteins using polyclonal COPS5 and monoclonal RanBP9 antibodies. Unlike the exogenously expressed proteins, the staining pattern was not so diffuse for endogenous RanBP9 and COPS5, both in HEK293 and NT2 cells. In both types of cells, the staining is markedly enriched in the cytoplasm (Fig. 3, *first* and *second columns*). DAPI staining was used to localize the nucleus (Fig. 3, *third column*). The merged images show an intense yellow color in the cytoplasm (Fig. 3, *fourth column*), suggesting that endogenous RanBP9 and COPS5 interact in the cytoplasm of both HEK293 and NT2 cells.

COPS5 Overexpression Strongly Increases β Site Cleavage of APP and Aβ Generation—The above demonstration of interaction between RanBP9 and COPS5 by immunoprecipitations and the colocalization by double immunofluorescence labeling
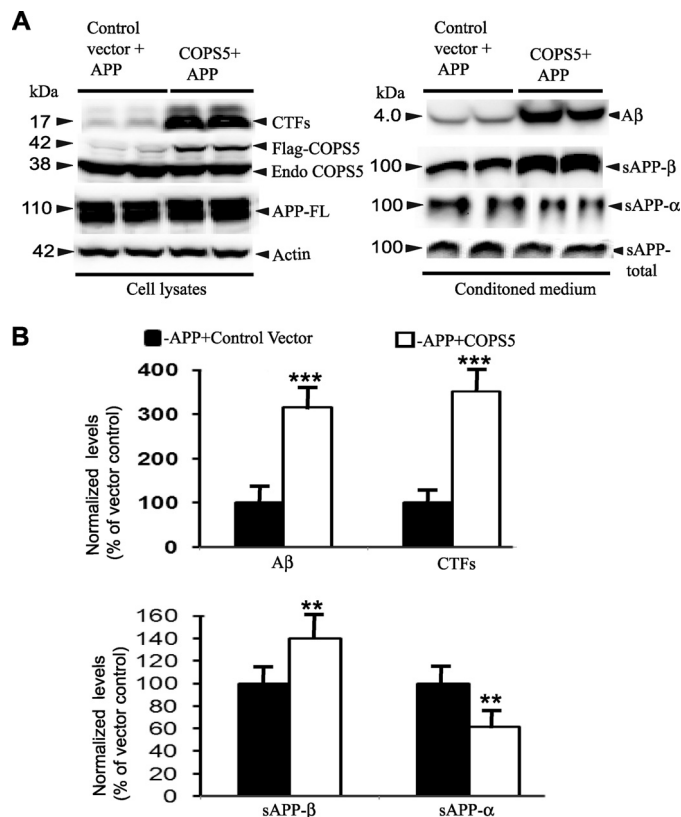

FIGURE 4. **COPS5 strongly increases levels of Aβ, CTFs, and sAPPβ in NT2 cells.** *A*, NT2 cells were transiently cotransfected with vectors encoding APP751wt and FLAG-COPS5, and the lysates were subjected to immunoblotting to detect CTFs, FLAG-COPS5, endogenous COPS5, APP holoprotein, and actin as a loading control. Conditioned medium was subjected to immunoprecipitations to detect total Aβ and also for immunoblot detection of sAPPs as indicated. *B*, ImageJ quantitation revealed that Aβ increased 3-fold, CTFs more than 3-fold, and sAPP-β by 40%, whereas sAPP-α levels were decreased by 39%. Protein levels were normalized to actin, and data are expressed as percentage change from vector-transfected controls and analyzed by Student's *t* test. Data are + S.E., and *n* = 4/group. **, *p* < 0.01; ***, *p* < 0.001.

suggests that COPS5-RanBP9 binding has a physiological significance. Next, to verify whether COPS5 influences APP metabolism and Aβ generation, as does RanBP9, we first quantified Aβ levels under COPS5 overexpression conditions in cell cultures. NT2 cells were transiently cotransfected with APP751 and FLAG-COPS5-FL. After 48 h, the conditioned media were recovered, and debris was removed by centrifugation at low speed. Aβ levels in the conditioned media were quantified by immunoprecipitations and SDS-PAGE electrophoresis as described previously by our laboratory (11). To minimize the variations in sample loading, we normalized the levels of Aβ, CTFs, and sAPPs to that of actin. Ab9 antibody (N terminus mAb, epitope Aβ1–16) was used to immunoprecipitate Aβ, and a combination of 6E10/82E1 antibodies were used for detection (11, 17, 18). The result revealed a 3-fold increase (*p* < 0.001) in Aβ levels and more than a 3-fold increase (*p* < 0.001) in the CTF levels upon COPS5 overexpression (Fig. 4, *A* and *B*). Detection with the COPS5 antibody confirmed the expression of exogenous FLAG-COPS5 only in the COPS5-transfected cells (Fig. 4*A*, *left panel*). The same antibody also detected endogenous COPS5 in all samples (Fig. 4*A*, *left panel*, *Endo COPS5*). Levels of APP holoprotein did not differ between the

COPS5-transfected and the control vector-transfected cells. However, quantitation of sAPPs from the conditioned media also revealed significant differences. sAPP-β levels were increased by 39% ($p < 0.01$), and sAPP-α levels were decreased by 40% in the COPS5-transfected NT2 cells compared with cells transfected with control vector (Fig. 4, *A* and *B*). Taken together, these results demonstrate that COPS5, like RanBP9, increases β site processing of APP at the cost of α-secretase, processing leading to increased levels of Aβ/sAPP-β and decreased levels of sAPP-α in the conditioned media.

COPS5 Is Essential for Aβ Generation in NT2 Cells—Given that COPS5 overexpression significantly increased the generation and secretion of Aβ, we next wanted to determine whether reducing the COPS5 protein levels would decrease Aβ levels. If COPS5 is essential for Aβ generation, then the absence of COPS5 should reduce Aβ levels. Indeed, we found a 54% ($p < 0.01$) reduction in Aβ levels, as determined by ELISA, and a 63% ($p < 0.01$) reduction in CTF levels, as determined by immunoblot analyses when COPS5 was knocked down using COPS5-specific synthetic siRNAs compared with scrambled control siRNAs (Fig. 5, *A* and *B*). COPS5 synthetic siRNAs visibly reduced COPS5 and RanBP9 protein levels compared with scrambled control siRNAs (Fig. 5*A*, *second* and *third rows*). Quantitation revealed a 75% ($p < 0.01$) reduction in COPS5 levels and a 35% ($p < 0.05$) reduction in RanBP9 levels (Fig. 5*C*). However, neither the APP holoprotein nor actin levels were altered (Fig. 5*A*, *fourth* and *fifth rows*), suggesting that the effect of COPS5 siRNA is specific and that the reduced Aβ levels are due to a reduction in the levels of COPS5 and protein. This confirms the regulatory role of COPS5 in Aβ generation.

To test whether reducing RanBP9 protein levels in the background of COPS5 overexpression would affect Aβ generation, we transiently cotransfected NT2 cells with APP751 and the control vector; APP751, FLAG-COPS5, and control siRNAs; and APP751, FLAG-COPS5, and RanBP9 siRNAs. In the presence of control siRNAs, COPS5 overexpression increased Aβ generation to 316% ($p < 0.001$) when compared with APP751-only-transfected cells (Fig. 5*D*). However, when RanBP9-specific siRNAs were cotransfected, the increase in Aβ levels was only 210% ($p < 0.01$) and, thus, reduced Aβ levels by 105%, which was statistically significant ($p < 0.001$). This suggests that COPS5-induced Aβ generation is probably through RanBP9.

COPS5 Promotes Stabilization of RanBP9 Protein—Because COPS5 is known to regulate the stability of several proteins, we first measured the steady-state levels of RanBP9 protein with or without COPS5 overexpression. We found a robust increase in the normalized (to actin) levels of both RanBP9-FL and the N-terminal proteolytic product, RanBP9-N60. RanBP9-FL was increased to 358% ($p < 0.01$), and RanBP9-N60 was increased to 248% ($p < 0.05$) in COPS5-transfected cells compared with control vector-transfected cells (Fig. 6, *A* and *B*). To test the effect of COPS5 overexpression on RanBP9 protein stability, we inhibited protein synthesis with cycloheximide (Fig. 6*C*). We transfected NT2 cells with RanBP9 with (Fig. 6*C*, *A lanes*) or without (*B lanes*) COPS5, followed by incubation with CHX and the cells were lysed at different time points. We demonstrated previously that RanBP9 has a half-life of about 1 h (10),
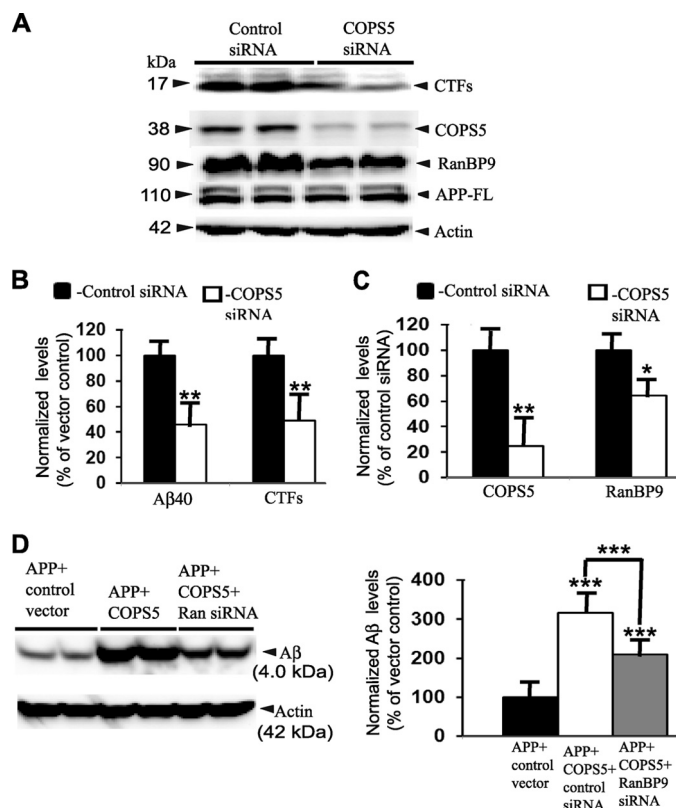

FIGURE 5. **Knockdown of COPS5 by siRNAs decreases Aβ40 and CTF levels in neuro-2A (N2A) cells.** *A*, N2A cells stably expressing APP695swe were transfected with siRNAs against either COPS5 or scrambled control siRNAs, and after 48 h, the lysates were immunoblotted to detect CTFs, COPS5, RanBP9, APP-FL, and actin. *B*, the conditioned media from the experiments in *A* were subjected to ELISA detection and quantitation of Aβ40. Compared with control siRNAs, COPS5 siRNAs reduced Aβ40 levels by 54% and CTF levels by 63%. *C*, quantitation of COPS5 levels by ImageJ revealed a 75% reduction and that of RanBP9 a 35% reduction in COPS5 siRNA-transfected cells compared with the controls. *D*, to examine the role of RanBP9 in COPS5-induced increased Aβ levels, NT2 cells were transiently transfected with APP751 plus control vector, APP751 plus FLAG-COPS5 plus control siRNAs, and, finally, APP751 plus FLAG-COPS5 plus RanBP9 siRNAs. Aβ quantitation in the conditioned media showed increased Aβ levels to 315% in the APP plus COPS5 plus control siRNA-transfected cells and a reduction to 210% when RanBP9 siRNAs were transfected. Protein levels were normalized to actin, and data are expressed as percentage change from controls and were analyzed by Student's t test or analysis of variance followed by Tukey-Kramer multiple comparison test. Data are + S.E., and $n = 4$. *, $p < 0.05$; **, $p < 0.01$; ***, $p < 0.001$.

and, therefore, we monitored transfected cells for up to 4 h. The immunoblot band intensities were measured and quantified at different time points for both RanBP9-FL and RanBP9-N60, revealing striking differences between vector controls and COPS5-transfected cells, especially at later time points (Fig. 6*C*). The analysis demonstrated that transfected RanBP9 has a half-life of about 1 h, consistent with our previous results (10). However, in the presence of COPS5, more intense bands of both RanBP9-FL and RanBP9-N60 were seen as late as 4 h after cycloheximide addition, by which time RanBP9 completely disappeared in the vector-transfected control cells (Fig. 6*C*). The data were normalized to actin levels, which remained stable at all times points tested in this study, even in the presence of cycloheximide, as reported previously (19). Normalized RanBP9 protein levels plotted against time are shown in Fig. 6*D*, which clearly indicates that the RanBP9 half-life is increased

A

COPS5 +RanBP9   Control Vect +RanBP9

90 kDa ►   ◄ RanBP9-FL
60 kDa ►   ◄ RanBP9-N60
42 kDa ►   ◄ Flag-COPS5
38 kDa ►   ◄ Endo. COPS5
42 kDa ►   ◄ Actin

B

■ -RanBP9 + Control   □ -RanBP9 + COPS5

RanBP9-FL/Actin (% of vector control)

RanBP9-N60/Actin (% of vector control)

C

Cycloheximide

Minutes ►   0   15   30   60   120   240
A B   A B   A B   A B   A B   A B

90 kDa ►   ◄ RanBP9-FL
60 kDa ►   ◄ RanBP9-N60
42 kDa ►   ◄ Flag-COPS5
38 kDa ►   ◄ Endo. COPS5
42 kDa ►   ◄ Actin

D

RanBP9-FL/Actin (% of 0 time point)

▲ -RanBP9 +COPS5
■ -RanBP9 +Control Vector
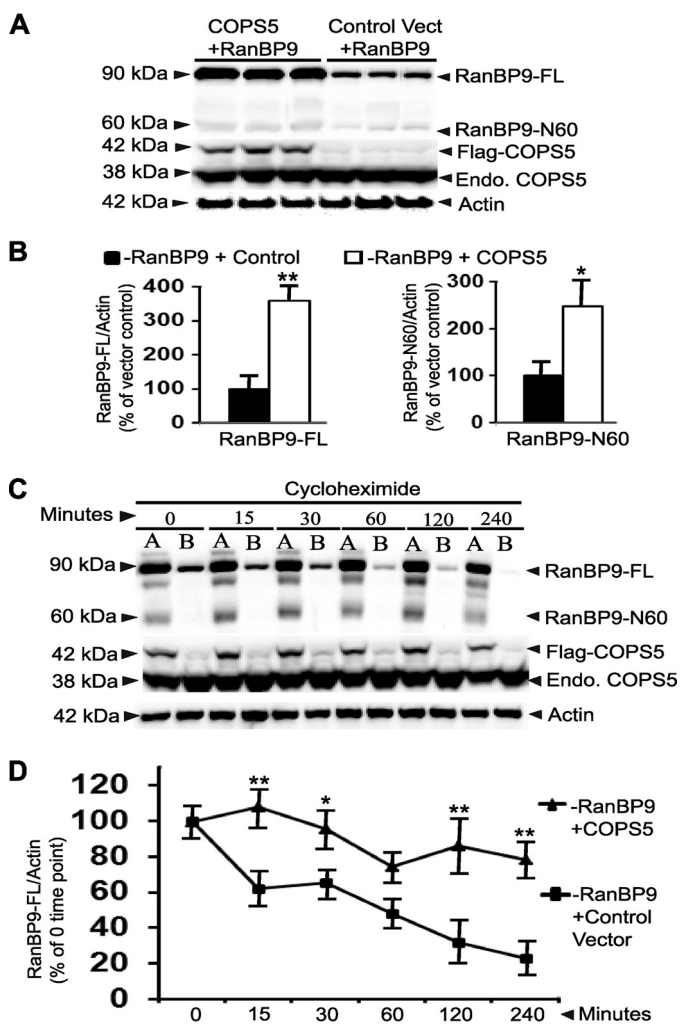
0   15   30   60   120   240 ◄ Minutes

FIGURE 6. **COPS5 robustly increases RanBP9 protein levels in NT2 cells.** *A*, NT2 cells were transiently cotransfected with vectors encoding GFP-RanBP9 plus either FLAG-COPS5 or control vector (*Control Vect*). After 48 h, the lysates were subjected to SDS-PAGE electrophoresis, and RanBP9, COPS5, and actin were detected using their specific antibodies. *B*, quantitation by ImageJ revealed more than a 3-fold increase in the levels of normalized (to actin) RanBP9-FL and more than a 2-fold increase in the normalized levels of the proteolytically cleaved form, RanBP9-N60. *C*, NT2 cells were transiently transfected with RanBP9-FL with (*A*) or without COPS5 (*B*) and were treated with cycloheximide (100 μg/ml) for the indicated time points. Monoclonal anti-RanBP9 antibody was used to detect RanBP9-FL and RanBP9-N60. Monoclonal COPS5 antibody detected both the exogenous FLAG-COPS5 and the endogenous (*Endo*) COPS5. Actin was used as a loading control. *D*, ImageJ-quantitated normalized levels of RanBP9-FL were plotted against time. Data were expressed as percentage change from vector controls and analyzed by repeated measures analysis of variance followed by Dunnett multiple comparison test. Data are + S.E., and *n* = 3. **, *p* < 0.01.

to > 4 h in the presence of COPS5 compared with a half-life of approximately 1 h without COPS5. These data demonstrate that the interaction with COPS5 leads to RanBP9 stabilization, which supports the observed increased steady-state level of RanBP9 in the presence of overexpressed COPS5.

COPS5 Levels Are Increased in AD Brains and APΔE9 Mouse Brains—To determine whether COPS5 levels were altered in Alzheimer's brains, we examined by immunoblotting COPS5 protein expression in the hippocampus from seven pathologically confirmed AD patients and age-matched normal controls (NC). The NC and AD brain tissues from both male and females were obtained from the Harvard Brain Tissue Resource Center.
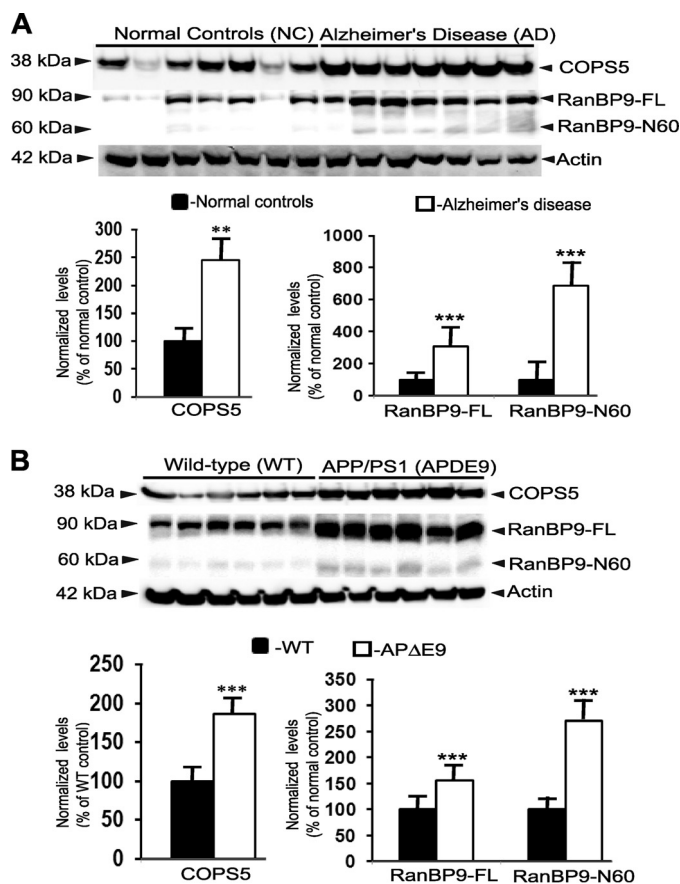
A

Normal Controls (NC)   Alzheimer's Disease (AD)

38 kDa ►   ◄ COPS5
90 kDa ►   ◄ RanBP9-FL
60 kDa ►   ◄ RanBP9-N60
42 kDa ►   ◄ Actin

■ -Normal controls   □ -Alzheimer's disease

Normalized levels (% of normal control)   COPS5

Normalized levels (% of normal control)   RanBP9-FL   RanBP9-N60

B

Wild-type (WT)   APP/PS1 (APDE9)

38 kDa ►   ◄ COPS5
90 kDa ►   ◄ RanBP9-FL
60 kDa ►   ◄ RanBP9-N60
42 kDa ►   ◄ Actin

■ -WT   □ -APΔE9

Normalized levels (% of WT control)   COPS5

Normalized levels (% of normal control)   RanBP9-FL   RanBP9-N60

FIGURE 7. **COPS5 protein levels are increased in AD brains and APΔE9 mice.** *A*, seven AD and seven age-matched NC brains were lysed in 1% Nonidet P-40 buffer, and equal amounts of ultracentrifuged lysates were subjected to SDS-PAGE electrophoresis and immunoblot detection of COPS5, RanBP9-FL, RanBP9-N60, and actin. ImageJ quantitation showed normalized (to actin) levels of COPS5 increasing more than 2-fold in AD brains compared with NC brains. RanBP9-FL levels increased to 307%, and RanBP9-N60 levels increased to 688% compared with NC brains. *B*, six APΔE9 brain samples from 12-month-old mice and six brain samples from age-matched WT mice were processed as in *A*, and protein bands were quantified by ImageJ. COPS5 levels were increased to 186% in APΔE9 mice compared with WT controls. Levels of RanBP9-FL increased to 155%, whereas those of RanBP9-N60 increased to 270% in APΔE9 mice compared with WT controls. Data are expressed as percentage change from controls and analyzed by Student's *t* test for significance. *n* = 7 (human brains) or *n* = 6 (mouse brains) + S.E. **, *p* < 0.01; ***, *p* < 0.001.

The age range of the NC subjects was 70–89 years, and the post-mortem interval was between 15–27.25 h. For AD patients, the age range was 69–93 years, and the post-mortem interval was between 17.58–30.16 h. The diagnosis of AD was confirmed in the post-mortem tissue by tau and plaque stainings by the tissue distributors. The COPS5 levels were increased to 244% (*p* < 0.01) in AD brains when compared with age-matched normal controls (Fig. 7*A*). Similarly, RanBP9-FL was increased to 307% (*p* < 0.001), and RanBP9-N60 was increased to 688% (*p* < 0.001) in AD brains compared with NC brains (Fig. 7*A*). To confirm the specificity of this increase, we also examined the levels of actin in the same samples and found no changes in the AD brains *versus* normal controls. In Fig. 7*A* we present the COPS5 and RanBP9 protein levels normalized to actin levels. Similarly, normalized levels of COPS5 quantified in 12-month-old APΔE9 mice in the C57BL/6 background showed an increase by 86% (*p* < 0.001) when compared with

age-matched WT controls also in C57BL/6 background (Fig. 7*B*). Consistent with the increased COPS5 levels, RanBP9-FL and RanBP9-N60 levels were also increased by 55% ($p < 0.001$) and 270% ($p < 0.001$), respectively, in the APΔE9 brains. Thus, increased COPS5 levels in the Alzheimer's brain may increase the levels of RanBP9 and, consequently, Aβ levels. Taken together, these data indicate that COPS5 may play a pathological role in AD.

DISCUSSION

In this study, we demonstrate that COPS5 is a novel RanBP9-binding protein. The interaction between RanBP9 and COPS5 was confirmed by coimmunoprecipitations in cultured cells as well as mouse brains. Additionally, both proteins showed an overlapping subcellular distribution pattern in non-neuronal as well as neuronal cell lines, further validating the interaction between the two proteins. Most importantly, the interaction between RanBP9 and COPS5 resulted in increased stability of RanBP9 protein, consequently leading to increased APP metabolism and Aβ generation. These data suggest that RanBP9-COPS5 interaction has a functional significance.

An indirect support for the interaction of RanBP9 with COPS5 comes from a previous study that showed both RanBP9 and COPS5 in the same fractions of a multiprotein complex of more than 440 kDa (14). The existence of both RanBP9 and COPS5 in the same protein complexes suggests that they may interact with each other and that such an interaction has functional significance. RanBP9 is a multimodular scaffold protein known to interact with a great variety of proteins in almost every subcellular compartment in the cell, including the plasma membrane (8). Like RanBP9 (20–22) COPS5 is also present in the cytoplasm, nucleus, and at the inner leaflet of the plasma membrane, especially when it is in the free form but not when bound to the COP9 signalosome (16, 23, 24), suggesting that both proteins might interact at more than one subcellular location. This is also supported by our double-labeling studies, which showed a yellow color in the merged images at multiple compartments, reflecting colocalization of endogenous RanBP9 and COPS5 in both non-neuronal and neuronal cells. The versatile nature of RanBP9 interaction with diverse proteins is believed to result in several multiprotein complexes involved in regulating many signaling pathways. The domain organization of RanBP9 includes the proline-rich domain, PRY, SPRY (SPla and the ryanodine receptor), LisH, and CTLH, which are all protein-protein binding domains that greatly increase the number of possible interactions of a wide variety of proteins with RanBP9 (8, 11), making it a perfect protein for scaffolding function. Our two-hybrid screen and domain-mapping experiments suggest that it is the LisH domain of RanBP9 that specifically interacts with COPS5. LisH domains are known to mediate dimerization and oligomerization of proteins as well as to affect protein half-life by binding to other proteins (25). Mutation of specific conserved amino acids within the LisH domain reduces the protein half-life (25). These data are consistent with our observation that COPS5 overexpression significantly increased RanBP9 stability, possibly through binding to the LisH domain of RanBP9.

COPS5 is known to affect the stability of several proteins. Previous studies reported that COPS5 binds several essential cell cycle regulatory proteins such as p27, p53, and Smad4, resulting in their degradation (26–29). By decreasing the stability of these proteins, COPS5 has been shown to play crucial roles in apoptosis and DNA checkpoint and damage repair (26–29). A more recent study also reported that COPS5 binds brain-specific kinase 2 (BRSK2) and promotes its degradation through the ubiquitin proteasome pathway, thereby regulating G_2/M cell cycle arrest (30). Although most protein interactions with COPS5 resulted in protein degradation, COPS5 interaction with RanBP9 rather stabilized the RanBP9 protein and increased its half-life. Similarly, COPS5 has been shown to directly bind and stabilize another protein, hypoxia-inducing factor 1α (31). Thus, COPS5 can increase the stability of its interacting protein, most likely through an action on the ubiquitin proteasome system.

COPS5 is evolutionarily conserved across a wide range of species ranging from plants, yeast, and mice to humans (23), and COPS5 deletion mice exhibit embryonic lethality (32), suggesting that COPS5 plays some fundamental function in the cell. A fraction of the COPS5 protein is present in a large molecular complex, the COP9 signalosome, which is largely present in the nucleus of cells. COPS5 integrated in this complex has a deneddylase activity toward Cullin-based ubiquitin ligases and, therefore, affects the ubiquitination of a large number of their targets. Of note, a relevant fraction of COPS5 can accumulate in the cytoplasm of cells in a COP9-unbound form. Although presumably this free form is responsible for many of the described protein interactions of COPS5, its biochemical function is still unclear. Although a substantial amount of COPS5 is expressed in the neurons and the brain, the role of COPS5 in the brain is completely unknown. Although most studies on COPS5 reported so far were on non-neuronal cells, a recent study found physical interaction between human serotonin receptor 6 (5-HT_6R), a G protein-coupled receptor, and COPS5 (33). In this study, siRNA-mediated down-regulation of COPS5 decreased the activity of 5-HT_6R by reducing its protein expression, suggesting that COPS5 is necessary to maintain the activity and expression of endogenous 5-HT_6R. In another recent study, COPS5 was detected within the huntingtin aggregates (34). These pieces of evidence implicate COPS5 to play important roles in the brain and neurological disorders. However, the exact function of COPS5, especially in the brain, remains largely undetermined.

Interestingly, some previous observations are consistent with our conclusion that COPS5 increases Aβ generation and contributes to AD pathogenesis. COPS5 knockdown reduces β-catenin levels (35), and multimodal interactions between APP, presenilin 1 (PS1), and β-catenin have been reported (36), suggesting that the COPS5-β-catenin pathway might also contribute to AD pathogenesis.

Because overexpression of COPS5 led to increased RanBP9 protein stability, increased COPS5 levels in Alzheimer's brains can be expected to increase RanBP9 protein levels in the Alzheimer's brain. Consistent with this prediction, here we found increased levels of both RanBP9-FL and RanBP9-N60 in Alzheimer's brains as well as APΔE9 transgenic mice. We also

demonstrated previously that RanBP9 protein levels were increased in J20 mice, also APP transgenic mice (37). We also demonstrated that RanBP9 scaffolds a tripartite protein complex by directly binding to LRP, APP, and BACE1, and enhances their interaction and Aβ generation (10, 11). Similarly, we have now demonstrated that COPS5 can also bind with APP, LRP, and BACE1. Further, RanBP9 accelerates endocytosis of APP, LRP, and β1-integrin by physically interacting with each one of them, thereby simultaneously regulating cell adhesion and Aβ generation (11, 37). Because endocytosis of APP and LRP is required for Aβ generation (38–40), COPS5-mediated increased Aβ generation may be the consequence of increased RanBP9 protein levels and APP/LRP endocytosis. Interestingly, we and others previously found COPS5 directly binding to LFA-1 (16, 41), and LRP is also known to bind to LFA (42). Thus, by physically binding to RanBP9 and LFA, COPS5 is likely a part of this protein complex formed by RanBP9. Our observation that both COPS5 and RanBP9 increase Aβ generation when overexpressed individually, together with a demonstration by others that both COPS5 and RanBP9 are present in the same protein complexes, clearly indicates that the RanBP9-COPS5 protein complex regulates Aβ generation. This is also supported by siRNA studies in which down-regulation of both RanBP9 and COPS5 independently reduced Aβ generation. Most importantly, RanBP9-specific siRNAs significantly reduced COPS5-induced increased Aβ levels, suggesting that both COPS5 and RanBP9 act in the same pathway. Thus, COPS5 is a novel RanBP9-interacting protein and, like RanBP9, COPS5 will also be an excellent therapeutic target if the role of COPS5 in the amyloidogenic processing of APP and Aβ is confirmed *in vivo*.

REFERENCES

1. Wimo, A., Winblad, B., and Jonsson, L. (2010) The worldwide societal costs of dementia. Estimates for 2009. *Alzheimer's Dement.* **6**, 98–103
2. Hardy, J., and Selkoe, D. J. (2002) The amyloid hypothesis of Alzheimer's disease. Progress and problems on the road to therapeutics. *Science* **297**, 353–356
3. Jonsson, T., Atwal, J. K., Steinberg, S., Snaedal, J., Jonsson, P. V., Bjornsson, S., Stefansson, H., Sulem, P., Gudbjartsson, D., Maloney, J., Hoyte, K., Gustafson, A., Liu, Y., Lu, Y., Bhangale, T., Graham, R. R., Huttenlocher, J., Bjornsdottir, G., Andreassen, O. A., Jönsson, E. G., Palotie, A., Behrens, T. W., Magnusson, O. T., Kong, A., Thorsteinsdottir, U., Watts, R. J., and Stefansson, K. (*2012*) A mutation in APP protects against Alzheimer's disease and age-related cognitive decline. *Nature* **488**, 96–99
4. Gatz, M., Reynolds, C. A., Fratiglioni, L., Johansson, B., Mortimer, J. A., Berg, S., Fiske, A., and Pedersen, N. L. (2006) Role of genes and environments for explaining Alzheimer's disease. *Arch. Gen. Psychiatry* **63**, 168–174
5. Tanzi, R. E. (2013) A brief history of Alzheimer's disease gene discovery. *J. Alzheimer's Dis.* **33**, 5–13
6. Bird, T. D. (2008) Genetic aspects of Alzheimer's disease. *Genet. Med.* **10**, 231–239
7. Kamboh, M. I., Demirci, F. Y., Wang, X., Minster, R. L., Carrasquillo, M. M., Pankratz, V. S., Younkin, S. G., Saykin, A. J., Alzheimer's Disease Neuroimaging Initiative, Jun, G., Baldwin, C., Logue, M. W., Buros, J., Farrer, L., Pericak-Vance, M. A., Haines, J. L., Sweet, R. A., Ganguli, M., Feingold, E., Dekosky, S. T., Lopez, O. L., and Barmada, M. M. (2012) Genome-wide association study of Alzheimer's disease. *Transl. Psychiatry* **2**, e117
8. Suresh, B., Ramakrishna, S., and Baek, K. H. (2012) Diverse roles of the scaffolding protein RanBPM. *Drug Discov. Today* **17**, 379–387
9. Arefin, A. S., Mathieson, L., Johnstone, D., Berretta, R., and Moscato, P. (2012) Unveiling clusters of RNA transcript pairs associated with markers of Alzheimer's disease progression. *PLoS ONE* **7**, e45535
10. Lakshmana, M. K., Chung, J. Y., Wickramarachchi, S., Tak, E., Bianchi, E., Koo, E. H., and Kang, D. E. (2010) A fragment of the scaffolding protein RanBP9 is increased in Alzheimer's disease brains and strongly potentiates amyloid-β peptide generation. *FASEB J.* **24**, 119–127
11. Lakshmana, M. K., Yoon, I. S., Chen, E., Bianchi, E., Koo, E. H., and Kang, D. E. (2009) Novel role of RanBP9 in BACE1 processing of amyloid precursor protein and amyloid β peptide generation. *J. Biol. Chem.* **284**, 11863–11872
12. Lakshmana, M. K., Hayes, C. D., Bennett, S. P., Bianchi, E., Reddy, K. M., Koo, E. H., and Kang, D. E. (2012) Role of RanBP9 on amyloidogenic processing of APP and synaptic protein levels in the mouse brain. *FASEB J.* **26**, 2072–2083
13. Nishitani, H., Hirose, E., Uchimura, Y., Nakamura, M., Umeda, M., Nishii, K., Mori, N., and Nishimoto, T. (2001) Full-sized RanBPM cDNA encodes a protein processing a long stretch of proline and glutamine within the N-terminal region, comprising a large protein complex. *Gene* **272**, 25–33
14. Zou, Y., Lim, S., Lee, K., Deng, X., and Friedman, E. (2003) Serine/threonine kinase Mirk/Dyrk1B is an inhibitor of epithelial cell migration and is negatively regulated by the Met adaptor Ran-binding protein M. *J. Biol. Chem.* **278**, 49573–49581
15. Lakshmana, M. K., Chen, E., Yoon, I.-S., and Kang, D. E. (2008) C-terminal 37 residues of LRP promote the amyloidogenic processing of APP independent of FE65. *J. Cell Mol. Med.* **12**, 2665–2674
16. Bianchi, E., Denti, S., Granata, A., Bossi, G., Geginat, J., Villa, A., Rogge, L., and Pardi, R. (2000) Integrin LFA-1 interacts with the transcriptional coactivator JAB1 to modulate AP-1 activity. *Nature* **404**, 617–621
17. Hayes, C. D., Dey, D., Palavicini, J. P., Wang, H., Araki, W., and Lakshmana, M. K. (2012) Chronic cladribine administration increases amyloid β peptide generation and plaque burden in mice. *PLoS ONE* **7**, e45841
18. Hayes, C. D., Dey, D., Palavicini, J. P., Wang, H., Patkar, K. A., Minond, D., Nefzi, A., and Lakshmana, M. K. (2013) Striking reduction of amyloid plaque burden in an Alzheimer's mouse model after chronic administration of carmustine. *BMC Med.* **11**, 81–96
19. Dugina, V., Zwaenepoel, I., Gabbiani, G., Clément, S., and Chaponnier, C. (2009) β and γ cytoplasmic actins display distinct distribution and functional diversity. *J. Cell Sci.* **122**, 2980–2988
20. Denti, S., Sirri, A., Cheli, A., Rogge, L., Innamorati, G., Putignano, S., Fabbri, M., Pardi, R., and Bianchi, E. (2004) RanBPM is a phosphoprotein that associates with the plasma membrane and interacts with the integrin LFA-1. *J. Biol. Chem.* **279**, 13027–13034
21. Valiyaveettil, M., Bentley, A. A., Gursahaney, P., Hussien, R., Chakravarti, R., Kureishy, N., Prag, S., and Adams, J. C. (2008) Novel role of the muskelin-RanBP9 complex as a nucleocytoplasmic mediator of cell morphology regulation. *J. Cell Biol.* **182**, 727–739
22. Poirier, M. B., Laflamme, L., and Langlois, M. F. (2006) Identification and characterization of RanBPM, a novel coactivator of thyroid hormone receptors. *J. Mol. Endocrinol.* **36**, 313–325
23. Chamovitz, D. A., Segal, D. (2001) JAB1/CSN5 and the COP9 signalosome. A complex situation. *EMBO Rep.* **2**, 96–101
24. Shackleford, T. J., and Claret, F. X. (2010) JAB1/CSN5. A new player in cell cycle control and cancer. *Cell Div.* **5**, 26–35
25. Gerlitz, G., Darhin, E., Giorgio, G., Franco, B., and Reiner, O. (2005) Novel functional features of the Lis-H domain. *Cell Cycle* **4**, 1632–1640
26. Tomoda, K., Kubota, Y., and Kato, J. (1999). Degradation of the cyclin dependent-kinase inhibitor p27kip1 is instigated by Jab1. *Nature* **398**, 160–165
27. Bech-Otschir, D., Kraft, R., Huang, X., and Henklein, P. (2001) COP9 signalosome-specific phosphorylation targets p53 to degradation by the

ubiquitin system. *EMBO J.* **20,** 1630–1639

28. Oh, W., Yang, M. R., Lee, E. W., Park, K. M., Pyo, S., Yang, J. S., Lee, H. W., and Song, J. (2006) Jab1 mediates cytoplasmic localization and degradation of West Nile virus capsid protein. *J. Biol. Chem.* **281,** 30166–30174

29. Wan, M., Cao, X., Wu, Y., and Bai, S. (2002) Jab1 antagonizes TGF-β signaling by inducing smad4 degradation. *EMBO Rep.* **3,** 171–176

30. Zhou, J., Wan, B., Li, R., Gu, X., Zhong, Z., Wang, Y., and Yu, L. (2012) Jab1 interacts with brain-specific kinase 2 (BRSK2) and promotes its degradation in the ubiquitin-proteasome pathway. *Biochem. Biophys. Res. Commun.* **422,** 647–652

31. Bae, M. K., Ahn, M. Y., Jeong, J. W., Bae, M. H., Lee, Y. M., Bae, S. K., Park, J. W., Kim, K.R., and Kim, K.W. (2002) Jab1 interacts directly with HIF-1 α and regulates its stability. *J. Biol. Chem.* **277,** 9–12

32. Tomoda, K., Yoneda-Kato, N., Fukumoto, A., Yamanaka, S., and Kato, J. Y. (2004) Multiple functions of Jab1 are required for early embryonic development and growth potential in mice. *J. Biol. Chem.* **279,** 43013–43018

33. Yun, H.-M., Baik, J.-H., Kang, I., Jin, C., and Rhim, H. (2010) Physical interaction of Jab1 with human serotonin 6 G-protein-coupled receptor and their possible roles in cell survival. *J. Biol. Chem.* **285,** 10016–10029

34. Cong, S. Y., Pepers, B. A., Zhou, T. T., Kerkdijk, H., Roos, R. A., van Ommen, G. J., and Dorsman, J. C. (2012) Huntingtin with an expanded polyglutamine repeat affects the Jab1-p27 (Kip1) pathway. *Neurobiol. Dis.* **46,** 673–681

35. Schütz, A. K., Hennes, T., Jumpertz, S., Fuchs, S., and Bernhagen, J. (2012) Role of CSN5/JAB1 in Wnt/b-catenin activation in colorectal cancer cells. *FEBS Lett.* **586,** 1645–1651

36. Chen, Y., and Bodles, A. M. (2007) Amyloid precursor protein modulates b-catenin degradation. *J. Neuroinflammation* **4,** 29–37

37. Woo, J. A., Jung, A. R., Lakshmana, M. K., Bedrossian, A., Lim, Y., Bu, J. H., Park, S. A., Koo, E. H., Mook-Jung, I., and Kang, D. E. (2012) Pivotal role of the RanBP9-cofilin pathway in Aβ-induced apoptosis and neurodegeneration. *Cell Death Differ.* **19,** 1413–1423

38. Bu, G., Cam, J., and Zerbinatti, C. (2006) LRP in amyloid-β production and metabolism. *Ann. N.Y. Acad. Sci.* **1086,** 35–53

39. Perez, R. G., Soriano, S., Hayes, J. D., Ostaszewski, B., Xia, W., Selkoe, D. J., Chen, X., Stokin, G. B., and Koo, E. H. (1999) Mutagenesis identifies new signals for β-amyloid precursor protein endocytosis, turnover, and the generation of secreted fragments, including Aβ42. *J. Biol. Chem.* **274,** 18851–18856

40. Koo, E. H., and Squazzo, S. L. (1994) Evidence that production and release of amyloid β-protein involves the endocytic pathway. *J. Biol. Chem.* **269,** 17386–17389

41. Perez, O. D., Mitchell, D., Jager, G. C., South, S., Murriel, C., McBride, J., Herzenberg, L. A., Kinoshita, S., and Nolan, G. P. (2003) Leukocyte functional antigen 1 lowers T cell activation thresholds and signaling through cytohesin-1 and jun-activating binding protein 1. *Nat. Immunol.* **4,** 1083–1092

42. Spijkers, P. P., da Costa Martins, P., Westein, E., Gahmberg, C. G., Zwaginga, J. J., and Lenting, P. J. (2005). LDL-receptor-related protein regulates β2-integrin-mediated leucocyte adhesion. *Blood* **105,** 170–177